New Phytologist

NODULES WITH ACTIVATED DEFENSE 1 is required for maintenance of rhizobial endosymbiosis in *Medicago truncatula*

Chao Wang[1], Haixiang Yu[1], Li Luo[2], Liujian Duan[1], Liuyang Cai[3], Xinxing He[1], Jiangqi Wen[4], Kirankumar S. Mysore[4], Guoliang Li[3], Aifang Xiao[1], Deqiang Duanmu[1], Yangrong Cao[1], Zonglie Hong[5] and Zhongming Zhang[1]

[1]State Key Laboratory of Agricultural Microbiology, College of Life Sciences and Technology, Huazhong Agricultural University, Wuhan 430070, China; [2]Shanghai Key Lab of Bio-energy Crops, School of Life Sciences, Shanghai University, Shanghai 200444, China; [3]National Key Laboratory of Crop Genetic Improvement, College of Informatics, Huazhong Agricultural University, Wuhan 430070, China; [4]Plant Biology Division, The Samuel Roberts Noble Foundation, 2510 Sam Noble Parkway, Ardmore, OK 73401, USA; [5]Department of Plant, Soil and Entomological Sciences and Program of Microbiology, Molecular Biology and Biochemistry, University of Idaho, Moscow, ID 83844, USA

Author for correspondence:
Zhongming Zhang
Tel: +86 27 8728 1687
Email: zmzhang@mail.hzau.edu.cn

Received: *10 March 2016*
Accepted: *13 April 2016*

New Phytologist (2016) **212:** 176–191
doi: 10.1111/nph.14017

Key words: defense-like responses, legume, *Medicago truncatula*, necrosis, nitrogen fixation, nodules, rhizobial endosymbiosis, *Tnt*-insertion mutant.

Summary

- The symbiotic interaction between legume plants and rhizobia results in the formation of root nodules, in which symbiotic plant cells host and harbor thousands of nitrogen-fixing rhizobia.
- Here, a *Medicago truncatula nodules with activated defense 1* (*nad1*) mutant was identified using reverse genetics methods. The mutant phenotype was characterized using cell and molecular biology approaches. An RNA-sequencing technique was used to analyze the transcriptomic reprogramming of *nad1* mutant nodules.
- In the *nad1* mutant plants, rhizobial infection and propagation in infection threads are normal, whereas rhizobia and their symbiotic plant cells become necrotic immediately after rhizobia are released from infection threads into symbiotic cells of nodules. Defense-associated responses were detected in *nad1* nodules. *NAD1* is specifically present in root nodule symbiosis plants with the exception of *Morus notabilis*, and the transcript is highly induced in nodules. *NAD1* encodes a small uncharacterized protein with two predicted transmembrane helices and is localized at the endoplasmic reticulum.
- Our data demonstrate a positive role for NAD1 in the maintenance of rhizobial endosymbiosis during nodulation.

Introduction

Successful interactions between rhizobia and legume roots result in formation of a new organ, the root nodule, where rhizobia convert atmospheric dinitrogen into organic nitrogen compounds in exchange for supply of carbon sources. During nodulation for the model legume plants *Medicago truncatula* or *Lotus japonicus*, rhizobia invade the root hairs, move through the root epidermis via the infection threads (ITs), and are released into host cells of the root cortex. Inside the infected cells, they are enclosed by the symbiosome membrane and differentiate into large, elongated bacteroids that are dedicated to nitrogen fixation. Successful invasion requires recognition of rhizobial nod factors (NFs) by receptor-like kinase complexes present in compatible host plants (Oldroyd, 2013). Afterwards, an array of symbiotic genes, including those involved in signal transduction, transcription regulation, cytoskeleton rearrangement, cell wall degradation and hormone homeostasis, are expressed to sustain chronic infection and nodule initiation (Desbrosses & Stougaard, 2011; Udvardi & Poole, 2013; Downie, 2014; Soyano & Hayashi, 2014). Root nodule symbiosis also can be established between the actinobacteria from the genus *Frankia* and actinorhizal plants (Svistoonoff *et al.*, 2014). Although the molecular mechanism of early symbiotic events is well understood in the *Rhizobium*–legume root nodule symbiosis, little is known about genes that function in the later stage of symbiosis after rhizobia are internalized into nodule cells and develop into nitrogen-fixing symbiosomes. Identification of new genes involved in the later stage will increase our knowledge of symbiosome development, maintenance of endosymbiosis and nitrogen fixation.

Pathogen-associated molecular patterns (PAMPs), recognized by transmembrane pattern-recognition receptors (PRRs) at the surface of plant cells, can trigger several early defense responses, including the production of reactive oxygen species (ROS) (Meng & Zhang, 2013; Muthamilarasan & Prasad, 2013). The best characterized PRRs include the flagellin receptor FLAGELLIN SENSING 2 (FLS2) and the chitin elicitor receptor kinase CERK1 (Gómez-Gómez & Boller, 2000; Miya *et al.*, 2007). To overcome the PAMP-triggered immunity, pathogens deliver effector proteins into the plant cell to suppress plant immunity. In return, plants have evolved diverse disease resistance (R) proteins (Qi & Innes, 2013), most of which belong to

the nucleotide-binding site–leucine-rich repeat (NBS-LRR) protein family, to interact with the bacterial effectors and activate effector-triggered immunity involving the large-scale activation of defense genes, hypersensitive response (HR) or HR-like cell death (Muthamilarasan & Prasad, 2013). In fact, early rhizobial infection on legume roots can also evoke plant innate immunity similar to that which occurs with pathogenic invasion. However, the host immunity is transient and suppressed during the process of infection and colonization by compatible rhizobia to avoid rejection of the rhizobia (Kouchi *et al.*, 2004; Boscari *et al.*, 2013).

A series of plant mutants and genes have been reported to be involved in the later stages of nodule and/or bacteroid development and differentiation in *M. truncatula*. Among them, *Numerous Infections and Polyphenolics/Lateral root-organ Defective* (*NIP/LATD*), *does not fix nitrogen 2* (*DNF2*), *Symbiotic Cysteine-rich Receptor-like Kinase* (*SymCRK*) and *Regulator of Symbiosome Differentiation* (*RSD*) have been shown to be associated with the maintenance of rhizobial endosymbiosis and, in addition, prevention of defense-like responses in nodules. Nodules formed on these mutants display defense-like responses leading to cell death that is distinguished with senescence of nodules (Bagchi *et al.*, 2012; Sinharoy *et al.*, 2013; Berrabah *et al.*, 2014a,b). Roles of preventing host defenses in nodules were further studied for the latter three genes (Berrabah *et al.*, 2015), suggesting that bacterial cell death is regulated by multiple steps after rhizobia are internalized into symbiotic cells. Prevention of defense responses in nodules could be regulated by both the rhizobial and host autologous systems (Gourion *et al.*, 2015), and is critical for the maintenance of rhizobial endosymbiosis and viability. Other mutants of *M. truncatula* with phenotypes of defense-like responses, such as NF0438, NF0359, NF2853, NF1859, NF0673, NF2811, NF5654, NF4608, NF1320, TRV36 and 7Y (Maunoury *et al.*, 2010; Pislariu *et al.*, 2012; Domonkos *et al.*, 2013), are likely to be very useful for characterization of genes involved in the maintenance of rhizobial endosymbiosis and prevention of defense-like responses. Discovery of other components in this process will help us understand how rhizobia are stably maintained and active in symbiotic cells.

The recently released genome sequence (Young *et al.*, 2011), plenty of transcriptomic resources (Benedito *et al.*, 2008; He *et al.*, 2009; Moreau *et al.*, 2011; Roux *et al.*, 2014) and large insertion mutant collections (Tadege *et al.*, 2008) have made *M. truncatula* a powerful model with which to study the *Rhizobium*–legume symbiosis through reverse genetics approaches. In *M. truncatula*, nodules develop to typically zoned indeterminate nodules (Vasse *et al.*, 1990), containing an apical meristematic zone I, a bacterial infection zone II, an interzone II–III where rhizobia have entered plant cells and begin to terminally differentiate involving cell elongation and genome amplification governed by plant nodule-specific cysteine-rich (NCR) peptides (Van de Velde *et al.*, 2010), a nitrogen-fixing zone III, and a senescence zone IV that is formed only in older nodules. The heterologous population of rhizobial cells in various developmental stages separated by easily discriminated zones enables subtle investigation of the function of a certain gene in the nodule symbiosis. Here, we present the functional characterization of a gene in the later stage of nodulation. We named it *Nodules with Activated Defense 1* (*NAD1*) because defense-like responses are rapidly and strongly activated in the mutant nodules. The *NAD1* gene encodes a novel peptide with two transmembrane domains and was highly expressed in nodules. Our data demonstrate a positive role of NAD1 in the maintenance of rhizobial endosymbiosis in nodules.

Materials and Methods

Plant growth, inoculation and bacterial strains

Wild-type (WT) *Medicago truncatula* Gaertn. ecotype Jemolong A17 and loss-of-function mutants (*dmi1-1*, *dmi2-1*, *dmi3-1*, *nfp-1*, *nsp1-1* and *nsp2-2*) were used for expression profile or promoter-*GUS* analysis. *Medicago truncatula* ecotype R108 and homozygous *nad1* mutants (*nad1-1* and *nad1-2*) were used for phenotype analysis. These two independent *Tnt1* (for *transposable element of Nicotiana tabacum cell type1*) insertion *nad1* mutant were isolated from the Noble Foundation *M. truncatula* mutant collection by a PCR-based reverse screening approach. Seeds were scarified for 2 min in H_2SO_4 followed by sterilization with 2.5% of active chlorine for 5–8 min. Surface-sterilized seeds were synchronized at 4°C in the dark for 2 d. Seeds were placed upside-down on N-free Fahraeus medium containing 1.2% agar (http://www.noble.org/MedicagoHandbook/) for hypocotyl elongation at 22°C in the dark for 12–16 h. Nine to 12 germinated seedlings were transferred to a 10 × 10 cm growth pot containing a 1 : 2 ratio of perlite : vermiculite supplied with half-strength Fahraeus medium. Plants were grown in a 16 h 24°C : 8 h 18°C, day : night regime of 40–60% relative humidity. After 4 d of growth, plants were inoculated with 50 ml (optical density at 600 nm (OD_{600}) = 0.02) of *Sinorhizobium meliloti* per pot. Different strains were used including a WT Sm2011 strain and a Sm2011 strain carrying the pXLGD4 plasmid containing a *ProHemA:lacZ* transcriptional fusion (Leong *et al.*, 1985). Liquid culture of *S. meliloti* (OD_{600} = 1.0) grown overnight in Tryptone Yeast (TY) medium was pelleted by centrifugation and resuspended in half-strength Fahraeus medium with 0.5 mM KNO_3. *Agrobacterium rhizogenes* strain MSU440 was used for hairy root transformation (Limpens *et al.*, 2004).

QRT-PCR analysis

Total RNA from roots and leaves was isolated using Trizol reagent (Invitrogen, Carlsbad, CA, USA) and total RNA from stems, flowers, nodules and pods was isolated from at least 20 mg fresh materials for each sample using Trizol Plants Total RNA Isolation Kit (TransGen Biotech, Beijing, China), which was optimized for total RNA isolation from plant materials containing abundant polysaccharides and polyphenol. Primescript RT Reagent kit (Takara Biotechnology, Dalian, China) was used to eliminate genomic contamination of total RNA and synthesize first strand cDNAs. Real-time quantitative reverse transcription

(qRT)-PCR was performed using the SYBR Select Master Mix reagent (ABI, Waltham, MA, USA). All PCR reactions were performed using an ABI ViiATM 7 Real-Time PCR System under a standard cycling mode. All of the expression levels were analyzed and normalized using the *Actin* gene, which is stably expressed in all plant tissues. At least two biological replicates and three technical replicates for each sample were performed. Primers are listed in Supporting Information Tables S1 and S2.

Plasmid construction

For promoter-*β-glucuronidase* (*GUS*) reporter analysis, a 912-bp promoter fragment immediately upstream of the start codon of *MtNAD1* was amplified from *M. truncatula* genomic DNA and cloned to the *Sal*I/*Sma*I site of pCAMBIA1391Z. For complementation analysis, genomic DNA containing the 912-bp promoter fragment and the *MtNAD1* coding region was amplified and used to replace the *Ubiquitin* promoter region at the *Pst*I/*Asc*I site of the vector pUBGFP, generating pUBGFP-*gMtNAD1*. In a similar way, genomic DNA containing the *Lotus japonicus* ecotype MG20 *NAD1* coding region and a 3113-bp promoter fragment was amplified and cloned to pUBGFP at the *Pst*I/*BamH*I site, generating pUBGFP-*gLjNAD1*. For expression of *NAD1* genes from *L. japonicus*, *Alnus glutinosa*, *Morus notabilis* and *Serratia* sp. H1n under the control of *MtNAD1* promoter, pUBGFP-*ProMtNAD1:LjNAD1*, pUBGFP-*ProMtNAD1:AgNAD1*, pUBGFP-*ProMtNAD1:MnNAD1* and pUBGFP-*ProMtNAD1:SeNAD1* were constructed using an overlapping PCR method. The 912-bp promoter fragment was fused to *LjNAD1*, *AgNAD1*, *MnNAD1* and *SeNAD1* coding sequence, respectively. *SeNAD1* coding sequence was synthesized and optimized for plant codon usage bias. The resultant fragments were cloned to pUBGFP at the *Pst*I/*Asc*I site. Green fluorescence protein (GFP) and flag tagged NAD1 plasmids were produced by PCR or overlapping PCR, and subcloned to pUBHyg or pUBGFP-3 × Flag, respectively. Primers are listed in Table S2.

Insertion mutant screening and genotyping

Tnt1 retrotransposon insertions in *MtNAD1* were screened using a nested PCR approach (Tadege *et al.*, 2008; Cheng *et al.*, 2014). Subsequent genotyping in the M2 generation progeny was performed using primers *Tnt1*-Fw and *MtNAD1*-Rv1 for the *nad1-1* allele and *Tnt1*-Rw and *MtNAD1*-Rv1 for the *nad1-2* allele (Table S2).

Acetylene reduction assay

Nitrogenase activity of nodulated roots, detached from intact plants, was measured by acetylene reduction activity (ARA) after incubation of three to five roots and 2 ml acetylene (C_2H_2) in a closed 20-ml vial at 28°C for 1 h. For each sample, at least 15 plants divided into three to four replicates were analyzed. Acetylene was measured in a GC-4000A gas chromatograph (Dongxi, Beijing, China).

Complementation of the *nad1* mutant phenotype

Hairy root transformation was conducted by a standard procedure (Medicago Handbook). After 6 d of co-cultivation of seedlings with *A. rhizogenes* carrying proper complementation constructs, seedlings were transferred to HRE (Hairy Root Emergence) medium (1.2% agar; *Lotus japonicus* Handbook, http://link.springer.com/book/10.1007/1-4020-3735-X) for hairy roots emergence for 8 d. GFP-positive roots were selected and all the GFP-negative roots were removed. Transformed plants were then transferred to growth pots and inoculated with *S. meliloti* strain 2011 after 5 d growth. The nodulation phenotype was examined 3–4 wk after inoculation.

Histochemical staining

Nodules were stained for GUS activity for 4–6 h as described previously (Wang *et al.*, 2015). Longitudinal 70-μm-thick sections of stained nodules were cut with a vibratome (VT1200S; Leica, Wetzlar, Germany) and embedded in 6% agarose in water. For toluidine blue staining, nodules were fixed overnight in 4% (w/v) paraformaldehyde in 1 × phosphate-buffered saline (PBS), pH 7.4, at 4°C after vacuuming for 5 min. Following dehydration in ethanol series, nodules were embedded in paraffin and cut to ultrathin sections (5 μm). Sections were fixed on a glass slide and treated in a series of decreasing ethanol concentrations. Samples were finally stained with 1% (w/v) of toluidine blue solution for 40 min followed by a wash with distilled water. Staining for *β-galactosidase* (*lacZ*) activity was performed as described (Wang *et al.*, 2015). To estimate H_2O_2 *in situ*, nodules were hand-sectioned using a double-edged razorblade. Sections were then rapidly immersed in 1 mg ml^{-1} of 3′,3′-diaminobenzidine (DAB) solution, vacuum-infiltrated for 2 min and then incubated for 2–3 h at 25°C. The accumulation of phenolic compounds was detected by the potassium permanganate staining as described (Bourcy *et al.*, 2013).

TUNEL assay

Nodules from WT or mutant plants were fixed in formalin-acetic-alcohol (50% ethanol, 5% acetic acid, 3.7% formalin) solution. Terminal deoxynucleotidyl transferase dUTP nick end labeling (TUNEL) assays were performed using an *in situ* DeadEnd Colorimetric TUNEL System (Roche, Basel, Switzerland) according to the manufacturer's instructions.

Microscopy

Nodules and transformed hairy roots were observed and photographed by a fluorescence stereo microscope (Olympus SZX16, Tokyo, Japan). Sections from GUS, toluidine blue, DAB and polyphenol staining, as well as TUNEL detection and unstained nodules, were observed and photographed using a light microscope (Nikon ECLIPSE 80i, Tokyo, Japan). Autofluorescence of phenolic compounds and subcellular localization were detected using an Olympus FV1000 confocal laser-scanning fluorescence

microscope. GFP fluorescence was excited at 488 nm and the emission was detected at 505–535 nm. Red fluorescence protein (RFP) and Cy3 fluorescence was excited at 559 nm, and emission wavelengths were detected at 560–615 nm for RFP and 560–650 nm for Cy3.

Electron microscopy

For transmission electron microscope (TEM) analysis, nodules at 5, 7, and 14 d post inoculation (dpi) were hand-sectioned longitudinally into the fixative solution containing 3% glutaraldehyde, 2% formaldehyde, 0.1 M phosphate buffer (pH 7.2), vacuum-infiltrated for 5 min, transferred to a fresh fixative solution for 1 h at 4°C and 1 h at 22°C. Nodules were subsequently rinsed three times for 15 min with 0.1 M phosphate buffer, fixed in 1% OsO_4 in 0.1 M phosphate buffer for 2 h at 20°C, and rinsed three times for 15 min with 0.1 M phosphate buffer. Nodules were then dehydrated in a series of increasing ethanol concentrations (50%, 70%, 80%, 90%, 95% and 100%) for 15 min. The ethanol was replaced with Epon 812 in two steps (acetone : Epon 812, ratio 1 : 1 for 24 h and Epon 812 for 24 h). Samples were then polymerized in Epon 812 for 48 h at 60°C. Sections (60–80 nm) were obtained and stained with saturated uranyl acetate in distilled water for 15 min at 18–22°C, followed by lead citrate for 15 min. Sections were dried overnight at room temperature and observed with an electron microscope (Hitachi U8010, Tokyo, Japan). For scanning electron microscopy (SEM), longitudinally hand-sectioned nodules were fixed using the method described earlier. Samples were coated with 8 nm gold and observed on a scanning electron microscope (Hitachi SU8010).

Alignment and phylogenetic analysis

Software TMHMM (http://www.cbs.dtu.dk/services/TMHMM/) was used for prediction of transmembrane domains. Full-length protein sequences were aligned using ClustalW, edited by BioEdit Sequence Alignment Editor, used to generate the phylogenetic tree using the UPGMA method of Mega4.0. NAD1 homologous sequences are listed in Table S3.

RNA-seq analysis

Two independent biological replicates were performed for RNA-sequencing (RNA-seq) analysis. For each replicate, WT and *nad1-1* nodules and nodule-stripped roots at 21 dpi were harvested. Total RNAs were isolated using Trizol Plants Total RNA Isolation Kit (TransGen Biotech). The quality and concentration of RNA samples were measured with an Agilent 2100 Bioanalyzer (Agilent Technologies, Santa Clara, CA, USA) on Agilent RNA Pico chips. Subsequent RNA-seq library was constructed and sequenced on an Illumina Hiseq 2000 platform with 100-nucleotide oriented paired-end reads (http://www.illumina.com/) by the Berry Genomics service (http://www.berrygenomics.com/En/Default.aspx). Approximately 4 Gb sequence data with over 20 million read pairs were obtained for each sample. Fastqc (http://www.bioinformatics.babraham.ac.uk/projects/fastqc/) was used to check the quality of raw fastq files and the first 12-bp reads was trimmed due to their wavy sequence content using Trimmomatic (Bolger *et al.*, 2014). Clean reads were mapped to *Medicago* reference genome (JCVI Mt 4.0, http://www.jcvi.org/medicago/) using Tophat with default parameters. Mapped reads (in .bam format) were ordered and converted to .sam format using samtools (Li *et al.*, 2009). Reads matching each reference gene were calculated by htseq-count using the parameter '-m union strand –no' in the default union counting model (Anders *et al.*, 2015). Read counts were then imported into R (http://www.r-project.org/, v.3.1.2) for normalization and differentially expressed transcripts (fold change ≥ 2, *P*-value ≤ 0.05) were determined using DEseq (Anders & Huber, 2010). Gene ontology (GO) term enrichment in each gene list was identified using GOseq with the Medicago GO term annotations.

Subcellular localization

Complemented nodules expressing NAD1-3 × Flag were hand-sectioned using a double-edged razorblade and used for *in situ* immune-localization according to the method described (Maunoury *et al.*, 2010). GFP tagged NAD1 was coexpressed with RFP tagged endoplasmic reticulum (ER) (RFP-VNX), Golgi (Manl-RFP) and PM (RFP-SCAMP1) marker in *Arabidopsis* protoplasts (Wang *et al.*, 2014).

Results

NAD1 encodes a novel protein with two transmembrane domains that is present only in nodulating plants, with the exception of *Morus notabilis*

A group of genes in legume plants was previously identified as having nodule-specific expression (Li *et al.*, 2012). Among them, a gene encoding a small membrane protein was further identified in *M. truncatula* (*MtNAD1*; GenBank accession no. KX034079). *MtNAD1* has no intron in the coding region and encodes a peptide of 96 amino acids. Similarly, its orthologs in other organisms do not contain an intron and the length of the predicted peptides is *c.* 100 amino acids (Fig. 1a; Table S3). Bioinformatic analysis revealed that MtNAD1 and NAD1-like proteins all possess two transmembrane domains, but do not contain an N-terminal secretory signal peptide. MtNAD1 sequence was used to search for homologous proteins in all available databases, and every resulting sequence was used to search again for new homologs until no more new sequences could be obtained. NAD1 homologous proteins were found only in eight higher plant species (Fig. 1a; Table S3), with only one copy per genome in *M. truncatula*, *Cicer arietinum*, *L. japonicus*, *Phaseolus vulgaris*, *Cajanus cajan*, *A. glutinosa*, *Casuarina glauca* and *M. notabilis*, and two per genome in *Glycine max*, an allotetraploid species. Among them, *M. truncatula*, *C. arietinum*, *L. japonicus*, *P. vulgaris*, *C. cajan* and *G. max* are leguminous plants, whereas *A. glutinosa* and *C. glauca* are actinorhizal plants. Except *M. notabilis*, all of these species are able to establish the root

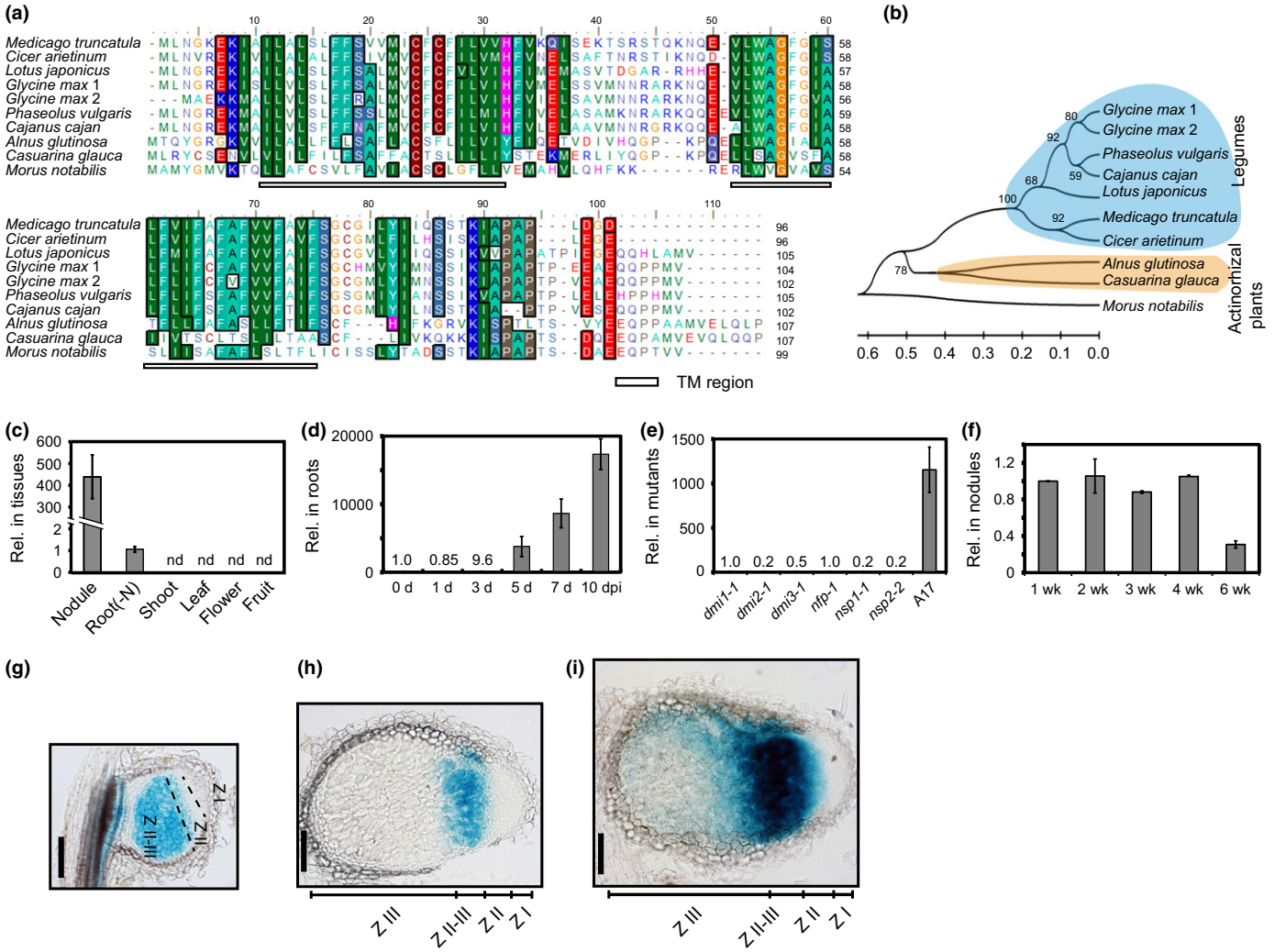

Fig. 1 Alignment and phylogenetic analysis of nodules with activated defense 1 (NAD1)-like proteins and *Medicago truncatula NAD1* expression. (a) Alignment of plant NAD1 and NAD1-like proteins. Conserved and similar residues are shaded by colors. Predicted transmembrane helices are marked by lines. Charged residues (lysine (K) and arginine (R) in blue, and glutamate (E) and aspartate (D) in red) with an irregular distribution were found on both sides of the two transmembrane helices. (b) Phylogenetic tree of NAD1-like proteins. Two clades representing legumes (blue) and actinorhizal (orange) plants are shaded with colors. Bootstrap values (%) obtained from 1000 trials are indicated at nodes. (c–f) Analysis of the *NAD1* transcript levels by quantitative reverse transcription polymerase chain reaction (qRT-PCR). Rel., relative expression levels; nd, not detected. Total RNAs from 3-wk-old nodules, nodule-stripped roots (root (-N)), shoots, leaves, young flowers and fruits was used for qRT-PCR (c). Total RNA from the control roots 0 d post inoculation (dpi) and roots inoculated with *Sinorhizobium meliloti* 2011 at different times (1–10 dpi) was used for qRT-PCR (d). Note that 5 dpi corresponds to the stage of rhizobial infection in the nodule primordia, and the first small nodule could be observed in our lab system. Symbiosis deficient mutants and the wild-type (WT) plants A17 were inoculated with *S. meliloti* 2011 and the roots were harvested 10 dpi (e). Nodules of the WT plants were harvested 1–6 wk post inoculation (wpi) with *S. meliloti* 2011 (f). Values were obtained from two to three biological replicates and error bars indicate ± SD (c–f). (g–i) Sections of (g) 1-wk- and (h, i) 3-wk-old nodules formed on transgenic hairy roots expressing the β-glucuronidase (GUS) reporter under the control of the *MtNAD1* promoter. Nodules were stained with GUS solution for (g, h) 4 h or (i) 6 h. Longitudinal sections of 70 μm in thickness were observed. Z, zone. Bars, 0.2 mm.

nodule symbiosis either with rhizobia or actinomyces. The phylogenetic tree of the NAD1 homologous proteins is characterized by the presence of two main clades, representing legumes and actinorhizal plants (Fig. 1b).

NAD1 is a nodule-specific gene that is expressed abundantly in interzone II–III

Gene expression atlas of *M. truncatula* and *L. japonicus* revealed nodule-specific expression patterns of *MtNAD1* and its ortholog *LjNAD1* (Fig. S1). To validate this, qRT-PCR was used to measure the expression level of *NAD1* in different tissues. The *NAD1* transcripts were essentially undetectable in aerial tissues and weakly detected in roots uninoculated with rhizobia, whereas nodules showed a high expression level of *NAD1* (Fig. 1c,d). In nodule-stripped roots 3 wk post inoculation (wpi), *NAD1* transcript was detected, which implied that the nodule-stripped root sample may contain nodule initiations which are hard to remove from roots (Fig. 1c). *NAD1* expression was elevated abruptly at 5 dpi and

continued to rise (Fig. 1d). In the *M. truncatula* mutants *dmi1-1*, *dmi2-1*, *dmi3-1*, *nfp-1*, *nsp1-1* and *nsp2-2*, which failed to establish symbioses, the induced expression of *NAD1* was abolished (Fig. 1e), suggesting the dependence of the induced *NAD1* expression on the establishment of nodule symbiosis. The expression of *NAD1* was sustained at high levels during the first 5 wpi, and started to decline in senescent nodules at 6 wpi (Fig. 1f). We also confirmed the nodule-specific expression pattern by the expression of the *GUS* reporter gene under the control of *MtNAD1* promoter in transgenic hairy roots. Histochemical staining analysis revealed specific expression of *NAD1* in nodules, particularly in interzone II–III (Fig. 1g,h). Prolonged staining of the nodules also indicated a weaker expression of *NAD1* in infection zone II and nitrogen-fixing zone III (Fig. 1i).

NAD1 is required for normal nodule development and symbiotic nitrogen fixation

In order to study the biological function of MtNAD1 protein, two independent *Tnt1*-insertion *nad1* mutants were identified from the Noble Foundation *M. truncatula* mutant collection by a PCR-based reverse screening approach (Tadege *et al.*, 2008; Cheng *et al.*, 2014). The line NF18553 (*nad1-1*) contains a *Tnt1* insertion in the 5′ untranslated region (5′-UTR), leading to *c.* 90% deduction of *NAD1* expression, whereas the line NF14356 (*nad1-2*) has the insertion in the open reading frame of *NAD1*, leading to a null mutant (Fig. 2a,b).

Homozygous *nad1* mutants of both lines exhibited chlorosis under symbiotic (nitrogen-free) growth conditions (Figs 2c, S2). However, the chlorosis symptom disappeared when mutant plants were grown in soil supplied with a nitrogen source (Fig. S2). Nodule number was increased in *nad1* mutant plants, likely due to a feedback regulation of the nodule number in nitrogen deficient plants (Fig. S2d). We could detect no nitrogenase activity in nodules of either mutants, suggesting a defect in nitrogen fixation of *nad1* nodules (Figs 2d, S2e). In WT plants, nodules became slightly pink at 7 dpi and turned fully pink at the late stage, an indication of high leghemoglobin (Lb) expression. By contrast, mutant nodules appeared white at 7 dpi and could not change to pink at the mature stage (Fig. 2e,f). Most of the mature nodules from mutant plants turned brownish in the basal regions proximal to the root, which has been suggested to be a result of defense-like pigment accumulation (Bourcy *et al.*, 2013). We observed that the brownish nodules could first be visible at 8 dpi.

Progenies of the *nad1*/+ heterozygous plants segregated in a canonical 3 : 1 ratio of plants with pink to plants with brownish nodules (212 : 71 for the *nad1-1* line, $\chi^2 = 0.0012$, $P = 0.0274$; 158 : 49 for *nad1-2*, $\chi^2 = 0.1948$, $P = 0.341$), suggesting a monogenic, recessive mutation. In segregated populations, all homozygous *nad1* mutant plants displayed brownish nodules and all heterozygous *nad1*/+ and WT plants produced functional, pink nodules (Fig. S3).

In order to further confirm that the *NAD1* gene caused the defective symbiotic phenotypes, we cloned the *MtNAD1* genomic DNA fragment, containing the *MtNAD1* native promoter and the coding region, into a binary vector. It was introduced to hairy roots of *nad1* plants. Four weeks after rhizobial inoculation, transgenic hairy roots produced functional, pink nodules that were normally elongated and similar in size and color to those in WT. As negative controls, transgenic hairy roots expressing the empty vector in *nad1* mutants produced dysfunctional brownish nodules (Fig. 2g,h). Internal structures as well as elongated bacteroid development were also rescued in the complemented nodules (Fig. 2i–k). In addition, only hairy roots expressing *NAD1* homolog from the legume plant *L. japonicus*, but not from the nonlegume plants *A. glutinosa* and *M. notabilis*, could rescue the nodule defects (Fig. 3). Taken together, these results unambiguously indicate that the *nad1* mutation is responsible for the observed phenotype of defective nodules in *nad1* plants.

NAD1 is required for rhizobial colonization in symbiotic cells in root nodules

In order to further investigate the biological function of *NAD1* during nodule development, semi-thin longitudinal nodule sections stained with toluidine blue were analyzed. Nodules of both *nad1* lines exhibited a rapid necrosis symptom of the two symbiotic partners: the host and the rhizobial cells (Fig. 4e–l). At 7 dpi, the plant cell wall of mutant nodules collapsed and bacteria were released from the symbiotic cells (Fig. 4e,f,i,j). The necrosis symptom deteriorated rapidly during the nodule development. No symbiotic cells filling with intact rhizobia could be observed in the mutant nodules 14 dpi. A few rhizobial cells could be observed only near IT-like structures and were likely to represent the bacteria that were just released from the IT (Fig. 4g,h,k,l). Using SEM, the necrosis phenotype could also be clearly observed (Fig. S4). When observed at 7 dpi, the necrosis symptom in *nad1-2* nodules was more severe than in *nad1-1* nodules (Fig. 4a,e,i), likely due to the fact that *nad1-2* is a null mutant, whereas *nad1-1* has a weakly leaky transcription.

In order to examine whether the symbiotic process in an early stage was altered in *nad1* plants, ITs were observed at 4 and 5 dpi. No difference was observed between the WT and mutants in aspects of IT development, rhizobial presence in ITs, rhizobial releasing from the ITs and the nodule primordium formation (Fig. S5), suggesting that MtNAD1 is not required for these earlier nodulation processes.

Bacteroid necrosis in *nad1* nodules

As no difference was detected in the infection process before rhizobia were released from ITs into the symbiotic cells, we asked if the defect in rhizobial infection took place immediately after rhizobia were released. Nodule primordia at 5 and 7 dpi were sampled for the ultrastructural analysis. In the WT nodules, rhizobia differentiated to the characteristic, elongated bacteroids and were enclosed by the symbiosome membrane (Figs 5a, S6a). As *nad1-2* displayed more rapid necrosis as described earlier, we focused our study on *nad1-1* nodules. In

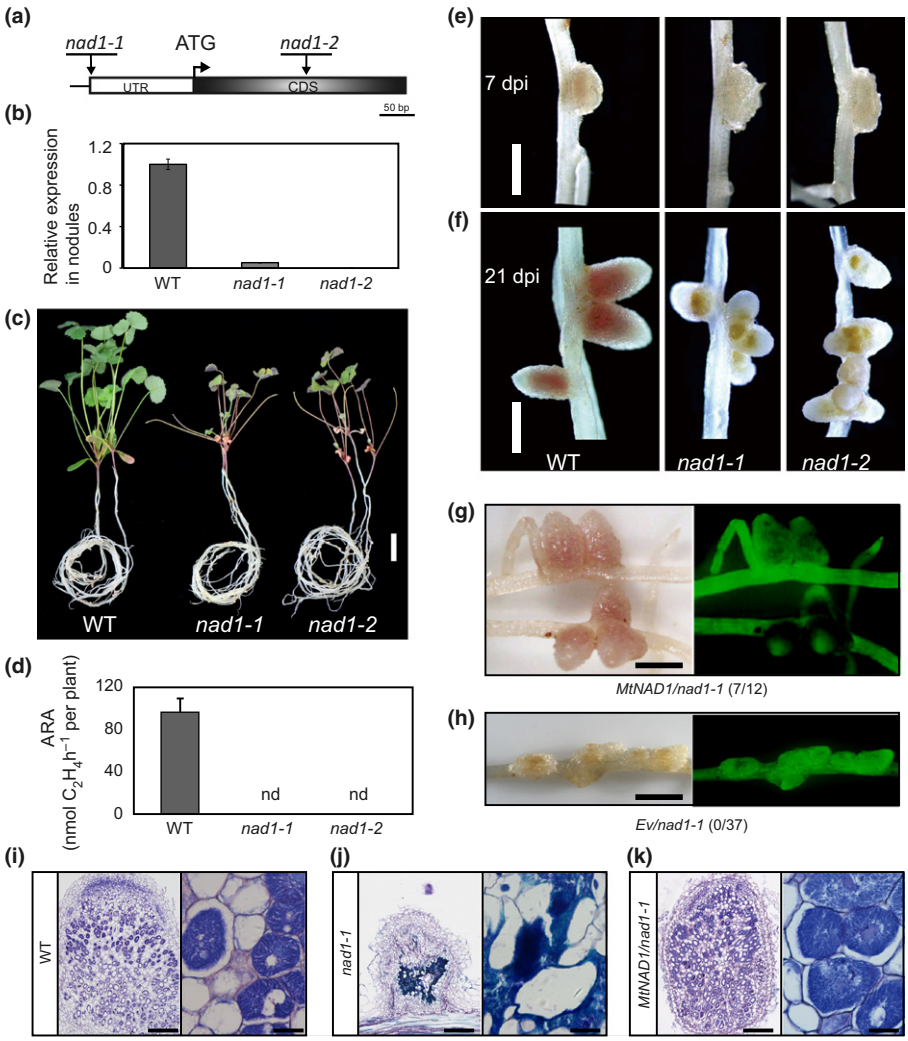

Fig. 2 Phenotype of *nodules with activated defense 1* (*nad1*) mutants and complementation by *NAD1*. (a) Insertion sites of *Tnt1* in the *NAD1* gene. The *MtNAD1* gene contains a coding region of 291 bp with no intron. The mutant *nad1-1* (NF18553) contains a *Tnt1* insertion in the 5′ UTR, −143 bp upstream of the translation start codon (ATG), whereas *nad1-2* (NF14356) has a *Tnt1* insertion in the coding region, 160 bp after the ATG. (b) The mRNA level of *NAD1* was quantified by quantitative reverse transcription polymerase chain reaction (qRT-PCR) in 3-wk-old nodules formed on wild-type (WT) *Medicago truncatula* R108 and mutant plants. Error bars indicate ± SD obtained from two biological replicates. (c–f) Plants of *nad1* mutants exhibited growth retardation that was associated with nitrogen deficiency (c). (d) Acetylene reduction assay (ARA) of nitrogenase activity was performed, revealing no nitrogen fixing activity of both *nad1-1* and *nad1-2* nodules at 3 wk post inoculation (wpi). nd, not detected. Error bars indicate ± SD obtained from three biological replicates. (e) At 7 d post inoculation (dpi) with *Sinorhizobium meliloti* 2011, nodules of *nad1* mutants remained white, whereas the WT nodules started to become pinkish, an indication of biosynthesis and accumulation of leghemoglobin. (f) In the mature stage of 21 dpi, *nad1* nodules exhibited brown pigmentation. No visible difference between *nad1-1* and *nad1*-2 was observed at the whole plant level and in pigmentation (f). (g–k) Functional complementation assays. (h) Transgenic hairy roots of *nad1-1* plants expressing the empty vector (*Ev*) produced defective nodules with pigmentation, whereas (g) the hairy roots expressing pUBGFP-*gMtNAD1* formed functional pink nodules at 28 dpi. Green fluorescence protein (GFP) expressed from the vector served as a selection marker for positive transformations. Values indicate the plants with pink nodules out of all transformed plants. (i–k) Sections of (i) WT, (j) mutant and (k) complemented nodules, indicating the endosymbiosis of rhizobia in mutant nodules were rescued. Bars: (c) 1 cm; (e–h) 1 mm; (i–k) 200 μm (left) and 20 μm (right).

nad1-1 nodules at 5 dpi (Fig. 5b), bacteroids remained small in size, similar to the free-living rhizobia. Some symbiosomes of *nad1* nodules appeared to contain two bacteroids, whereas symbiosomes of WT nodules had only one elongated bacteroid (Fig. 5a,b). In *nad1-1* nodules at 7 dpi, we could clearly identify the degradation or necrosis of the host cells and bacteroids (Figs 5c, S6b–d). Moreover, the peribacteroid space was enlarged and partially fused between two symbiosomes (Fig. S6c). In the magnified views, the cell wall of the bacteroid seemed to be untidy, possibly due to degradation (Fig. 5e,f). Chromatin condensation was also clearly observed in the necrotic bacteroid (Fig. 5f). In necrotic host cells, symbiosomes were disrupted and bacteroid necrosis are more severe (Fig. 5c, arrow). Besides the necrotic phenotypes, we also found abnormal and swollen mitochondria with indistinct inner membranes, suggesting a dysfunction of the mitochondria in *nad1* nodule cells at 5 dpi, whereas few such mitochondria could be observed in WT nodules at this stage (Figs 5d, S6f). No differences in nodules were observed regarding other organelles, including Golgi and ER, between *nad1* mutant and WT plants.

(a)

Mutant genotype	Constructs	Plants with pink nodules/total plants	Pink nodules per plant
nad1-1	*Ev*	0/37	-
nad1-2	*Ev*	0/6	-
nad1-1	*gMtNAD 1*	7/12	5.6
nad1-2	*gMtNAD 1*	6/11	6.2
nad1-1	*gLjNAD 1*	8/12	4.4
nad1-2	*gLjNAD 1*	2/7	4
nad1-1	*ProMtNAD1:LjNAD1*	7/10	3.3
nad1-1	*ProMtNAD1:AgNAD1*	0/30	-
nad1-1	*ProMtNAD1:MnNAD1*	0/29	-

(b)

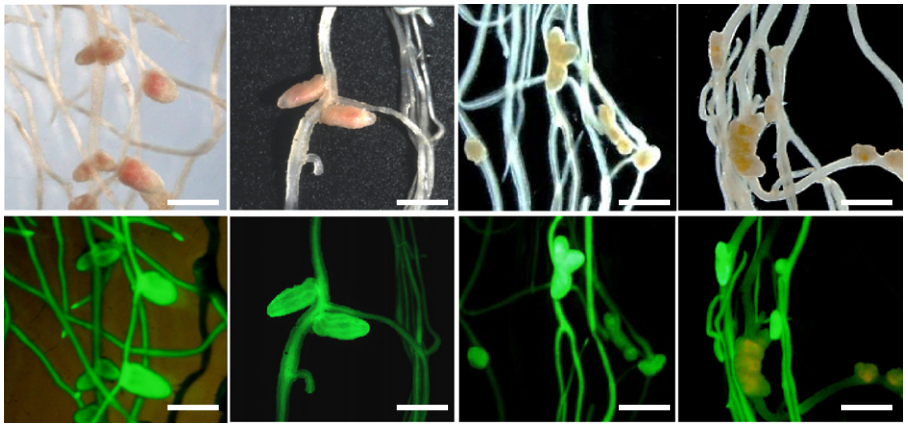

Fig. 3 Complementation of *nad1-1* plants by *nodules with activated defense 1* (*NAD1*) and *NAD1*-like genes. (a, b) NAD1-like genes from *Lotus japonicus*, *Alnus glutinosa* and *Morus notabilis* were used for complementation assays in *nad1* mutant plants. Nodule phenotype was observed at 28 d post inoculation (dpi) with *Sinorhizobium meliloti* 2011. Green fluorescence protein (GFP) expressed from the construct was used as a selection marker for transformations. Numbers indicate the plants with pink functional nodules out of all transformed plants. Bars, 2 mm.

Defense-like responses in *nad1* nodules

In order to assess the defense-like response levels in *nad1* nodules, we measured the contents of phenolic compounds, hydrogen peroxide (H_2O_2) content, and the degrees of DNA fragmentation in the WT and *nad1* nodules. In *nad1* nodules, autofluorescence of phenolic compounds became detectable at 7 dpi and continued to increase to 10 dpi when the brown pigments began to accumulate at the root proximal region of nodules (Fig. 6a–i). This observation suggests that the brownish *nad1* nodules might be the result of the accumulation of phenolic compounds or their conjugate products. The presence of phenolic compounds was further confirmed with the potassium permanganate staining (Figs 6j,k, S7). We compared the defense responses of *nad1* nodules with *dnf2* nodules, another mutant with defense-like responses in nodules (Bourcy *et al.*, 2013), in our laboratory system, and showed a similar degree of necrosis (Fig. S8). In contrast to the WT nodules, *nad1* nodules contained higher concentrations of H_2O_2, especially in the similar region where brown pigments accumulated (Fig. 6l,m). Additionally, strong staining for DNA fragmentation, a result from cell death signaling cascades, was observed in both plant nuclei and rhizobia (Figs 6n,o, S7).

Gene reprograming by *nad1* mutation

In order to investigate the dynamic transcriptional reprogramming in *nad1* mutant nodules, differentially expressed genes (DEGs) in root nodules were analyzed (fold change ≥ 2, P-value ≤ 0.05) using an RNA-seq technique. DEGs between WT nodules (WT Nod) and WT nodule-stripped roots (WT R) revealed that a large number of genes (7975) displayed differential expression in WT Nod vs WT R, which is consistent with a previous report that has similar number (10 805) of DEGs (Boscari *et al.*, 2013). Among DEGs in WT Nod vs WT R, 49% (3884) of genes were upregulated and the rest (4091) were downregulated (Table S4). Similarly, in *nad1-1* mutant nodules (mut Nod) vs WT Nod, 55% (4019) were upregulated and 45% (3253) were downregulated (Table S5). We focused on the gene families representative of the interesting transcriptional reprogramming from

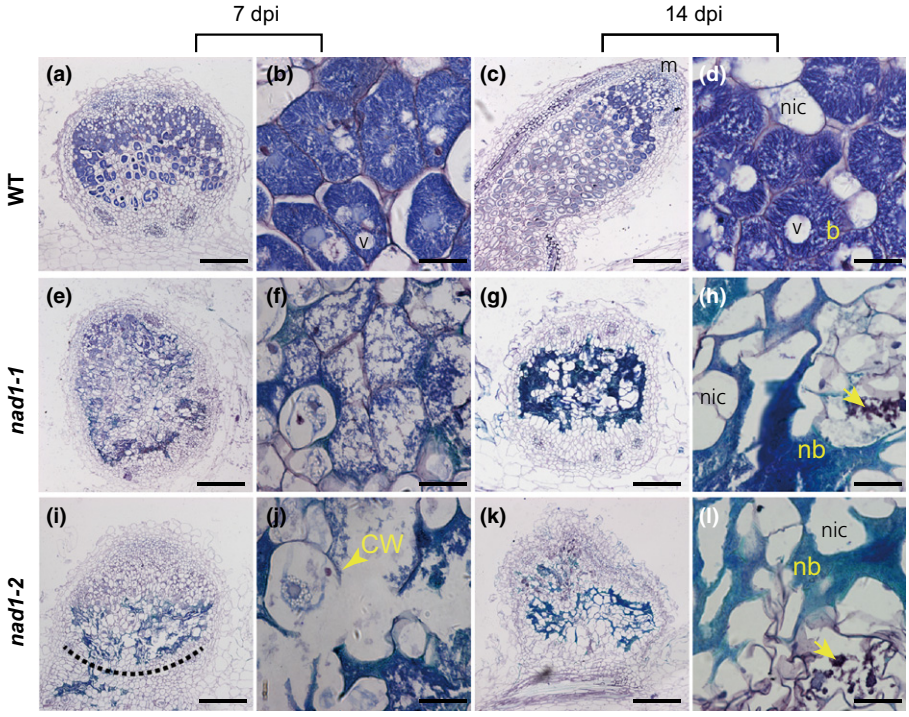

Fig. 4 Defective rhizobial endosymbiosis of *nad1* nodules. (a–d) The wild-type (WT) *Medicago truncatula* R108 nodules developed cylindrical nodules with an active apical meristem (a, c). Symbiotic cells were filled with symbiosomes that contained differentiated, elongated bacteroids (b, d). Magnified views of (a, c) are shown in (b, d). m, meristem; v, vacuole; b, bacteroid. (e–l) Inside the symbiotic cells of *nad1* nodules, rhizobia started to degrade at 7 d post inoculation (dpi) and were reduced to remnants by 14 dpi. (f, h, j, l) Symbiosomes of *nad1* nodules disintegrated and the cell wall of symbiotic cells were partially degraded at 14 dpi. (g, k) No typical apical meristems were visible in *nad1* nodules at 14 dpi. Magnified views of (e, g, i, k) are shown in (f, h, j, l). nb, necrotic bacteroids; CW, cell wall; nic, noninfected cell. Arrowheads indicate IT-like structures. Bars: (a, c, e, g, i, k) 200 μm; (b, d, f, h, j, l) 20 μm.

the 'symbiosis' features in WT nodules to the 'defense' features in mutant nodules. It revealed that defense-related gene families were largely repressed and even switched-off in WT Nod vs WT R (Fig. 7a), but were elevated in mut Nod vs WT Nod.

We selected 33 genes, including those previously revealed to be involved in defense or symbiosis processes in *M. truncatula* or other plant species, for the further qRT-PCR assay. Total RNA was isolated from nodules resampled from both *nad1-1* and *nad1-2* lines (Fig. 7b). Although *Defective in Nitrogen Fixation 1* (*DNF1*), *DNF2* and *SymCRK* (Wang *et al.*, 2010; Bourcy *et al.*, 2013; Berrabah *et al.*, 2014b) were not detected as DEGs in the RNA-seq data, their expression levels were reduced in the qRT-PCR results. All other genes exhibited similar expression patterns with the RNA-seq results (Fig. 7b; Table S1). The upregulated genes in mut Nod vs WT Nod included those related to plant defense, HR and protection against oxidative stress. However, among the transcriptionally repressed genes in mut Nod vs WT Nod, there were genes related to carbon source transport, nitrogen fixation, auxin transport, and development of ITs, nodules and bacteroids. The large scale of transcription reprogramming in the late stage of nodulation could be a secondary/indirect effect by misregulated rhizobial endosymbiosis in *nad1* mutants. We further investigated the expression patterns in 7-d-old nodule primordia before obvious defense symptom became visible (Fig. 7c). The defense-related genes *respiratory burst oxidase homologues* (*Rboh*), *pathogenesis-related protein 10* (*PR10*), *Chitinase, vacuole processing enzyme* (*VPE*), *NBS-LRR, resistance* gene (*R*) and *non-race-specific disease resistance 1* (*NDR1*) were found to be significantly induced, and genes related to nodule endosymbiosis, such as *symbiotic sulfate transporter* (*MtSST1*, the ortholog of *LjSST1*), *Lb* and *NCR* were repressed. Genes including *NODULE INCEPTION* (*MtNIN*), *nodulation pectate lyase* (*MtNPL*), and *Ethylene response factor* (*ERF*) *required for nodulation 1* (*MtERN1*) that are required for development of ITs and nodule primordia were not significantly repressed at this stage, which is consistent with the observation that the ITs and nodule primordium development were not altered in *nad1* nodules. Our results suggested a rapid activation of plant defense-related genes after nodule initiation in *nad1* mutants.

Localization of NAD1 protein

In order to further understand the function of NAD1 in nodules, we studied the subcellular localization of NAD1. We introduced flag-tagged NAD1 to *nad1* hairy roots. The restored functional nodules were sampled for *in situ* immunofluorescence assay using an anti-flag antibody. NAD1 signals displayed numerous and elongated structures, presumably the ER, closely associated with symbiosomes (Fig. 8a,b). No signals were observed in the WT control nodules, suggesting that they were specific signals in nodules expressing flag-tagged NAD1 proteins. ER localization was further demonstrated by co-localization of GFP-fused NAD1, NAD1-GFP, with an ER marker protein (RFP-VNX) in *Arabidopsis* protoplasts (Fig. 8c–e).

Discussion

Legumes are set apart from other plant species because of their ability to establish an efficient symbiotic interaction with rhizobia in a specialized nodule organ, and have become a good model with which to study plant–microbe interactions with either beneficial or deleterious effects. Legumes possess 'special' genes in their genomes, which are specifically evolved for legume-specific functions including nodulation and biological nitrogen fixation

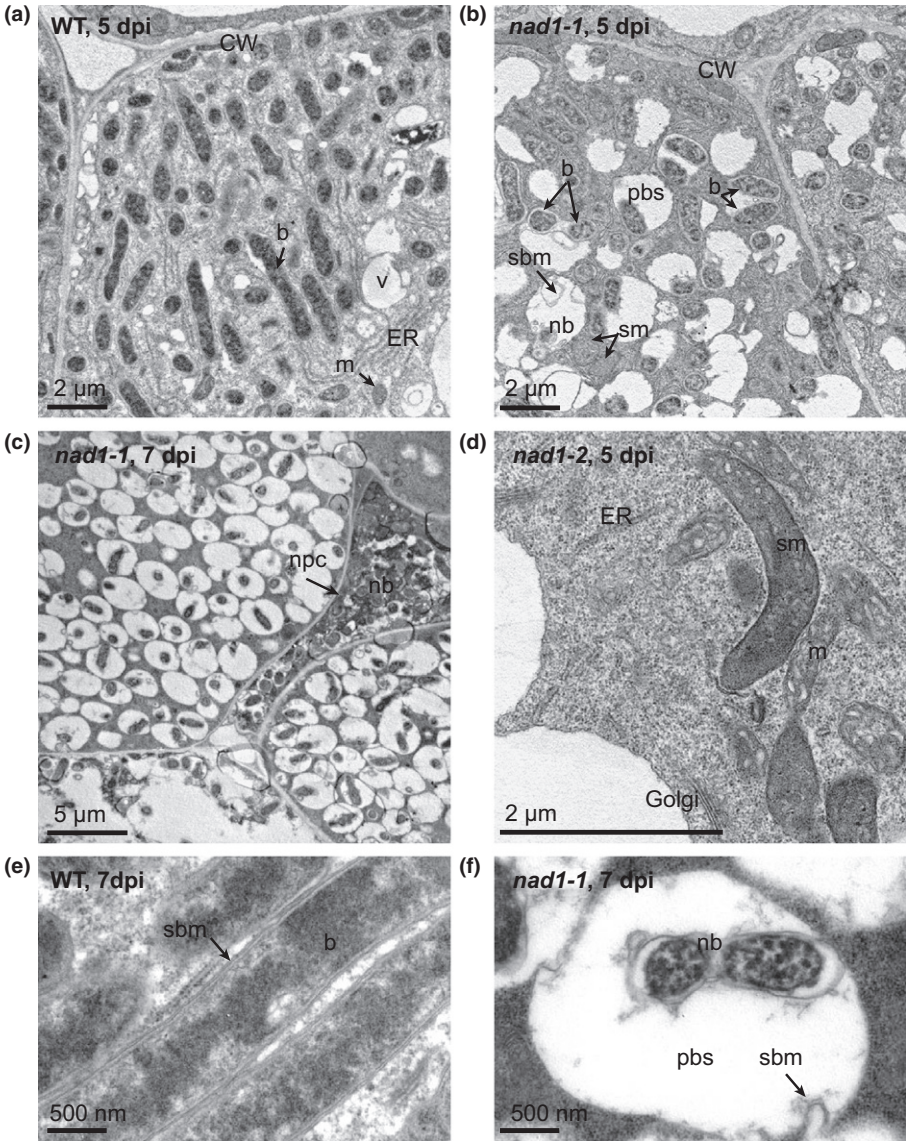

Fig. 5 Ultrastructures of the *nodules with activated defense 1* (*nad1*) nodules. Transmission electron microscope (TEM) images of nodules of the wild-type (WT) *Medicago truncatula* R108, *nad1-1* and *nad1-2* at 5 and 7 d post inoculation (dpi). (a) Rhizobia in the WT nodules differentiated to elongated bacteroids. (b) In *nad1-1*, peribacteroid spaces were enlarged, and some symbiosomes might contain two bacteroids. (c) Necrosis of both plant cells and bacteroids occurred in *nad1-1* nodules, and (d) swelling mitochondria with indistinct cristae were visible. (e, f) Bacteroids and the necrotic bacteroids in the (e) WT and (f) *nad1-1* nodules at 7 dpi. Chromatin condensation was observed in bacteroids in mutant nodules. b, bacteroid; v, vacuole; CW, cell wall; ER, endoplasmic reticulum; sbm, symbiosome membrane; pbs, peribacteroid space; npc, necrotic plant cell; nb, necrotic bacteroid; m, mitochondrion; sm, swollen mitochondrion.

(Graham *et al.*, 2004). Nevertheless, most of the genes involved in the hallmark legume functions are believed to be recruited from pathways shared with nonlegumes, especially the 'common signaling pathway' genes shared with the ancient arbuscular mycorrhizal symbiosis (Banba *et al.*, 2008; Markmann & Parniske, 2009; Oldroyd, 2013). Thus, uncovering the 'special' genes and their functions will facilitate the research of legume biology and increase our knowledge of the evolution of nodule symbiosis. Based on the genome and transcriptome information, we identified *MtNAD1* as an example of the 'special' genes. *NAD1* homologs exist in legumes and actinorhizal plants that could form nitrogen fixation nodules with rhizobia and *Frankia*, respectively. The *NAD1*-like cDNA from both actinorhizal plants, *A. glutinosa* and *C. glauca*, was isolated from the cDNA libraries of nodules 3 wk after inoculation with *Frankia* (Table S3), suggesting abundant expression of *NAD1* in root nodules of actinorhizal plants. No *NAD1*-like sequence was found in other plant species that could not form nitrogen fixation nodules, except *M. notabilis*, the reason for which remains unclear. Analysis of functional complementation revealed that *NAD1* genes from nonlegumes could not rescue the nodulation defect of *Mtnad1* mutant plants (Fig. 3), indicating that *NAD1* genes have evolved a specific function for accommodation in specific symbiosis systems. Searching from all released genome databases, we found other *NAD1*-like sequences in microbes with similar transmembrane topology of two transmembrane domains and distribution of charged residues (Table S3). The only microbe genera possessing *NAD1*-like genes are *Serratia* sp. and *Pantoea* sp., which are known to comprise species that are involved in plant–microbe interactions and nitrogen-fixing (Gyaneshwar *et al.*, 2001; Loiret *et al.*, 2004; Sandhiya *et al.*, 2005). However, expression of the microbial *Serratia* sp. H1n *NAD1*-like gene under the control of *MtNAD1* promoter does not rescue the defects of *nad1* mutant nodules (Fig. S9), suggesting that plant NAD1 homologs have evolved unique features. In consideration of its presence in nodule symbiosis plants, it will be interesting in

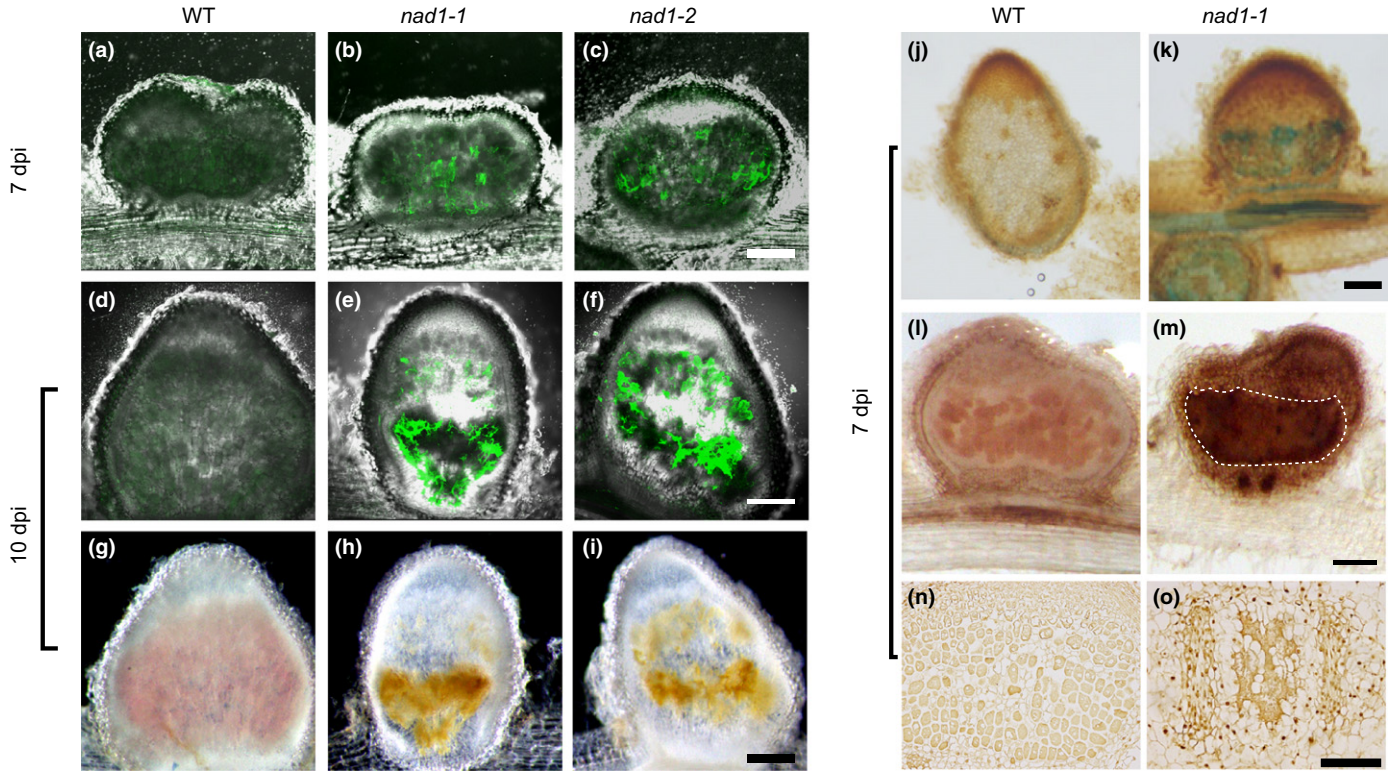

Fig. 6 Accumulation of phenolic compounds and pigments in the *nodules with activated defense 1* (*nad1*) nodules. (a–f, j, k) Phenolic compounds, (g–i) brown pigments, (l, m) hydrogen peroxide (H_2O_2) and (n, o) DNA fragmentation were detected and compared in the wild-type (WT) *Medicago truncatula* R108 and *nad1* nodules inoculated with *Sinorhizobium meliloti* 2011. (a–f) Autofluorescence of phenolic compounds detected under the green fluorescent protein (GFP) channel in *nad1* nodules emerged in the nodule primordia at 7 d post inoculation (dpi) (b, c) and became stronger at 10 dpi (e, f), as compared with that in the WT nodules (a, d). Under a light microscope, (g) the WT nodule appeared as pink due to leghemoglobin accumulation, whereas (h, i) *nad1* nodules accumulated brown pigments at the nodule region proximal to the root. (d–i) The autofluorescence signal and pigmentation overlapped with each other. (j, k) Phenolic compound staining for the WT and *nad1-1* nodules. (l, m) High concentrations of H_2O_2 were detected in the entire section of *nad1-1* nodules at 7 dpi. The highest concentration of H_2O_2 was found in the similar nodule region, highlighted by the dashed outline, where the phenolic autofluorescence and brown pigments were detected. This nodule region corresponded to the zone where rhizobia are released from the infection threads (ITs) and active endosymbiosis takes place. (n, o) DNA fragmentation, shown in brown signals, of both plant nuclei and rhizobia was detected by the TUNEL assay in *nad1-1* nodules, but not in the WT nodules. Bars, 0.2 mm.

future to investigate whether *Parasponia*, an exclusive nonlegume nodule symbiosis plant, has a *NAD1*-like gene or not.

The establishment and maintenance of the *Rhizobium*–legume symbiosis comprises a sequence of highly regulated events involving the two partners. One of the best known characteristics of these events is the suppression of plant defense responses to avoid rejection of the invading rhizobia. How rhizobia use signal molecules to evade host defense has been discussed in previous publications (Soto *et al.*, 2009; Saeki, 2011; Hayashi & Parniske, 2014). Here, we described a *M. truncatula nad1* mutant that forms nitrogen-fixation deficient nodules with defense-like responses. The time-course analysis of nodules at 4–7 dpi clearly indicated that the defect in the mutant happens immediately after rhizobia are released from ITs into host cells (Figs 4–6), which was consistent with the *NAD1* expression profiles (Fig. 1). Compared with the mutants that have previously been described to produce defense-like responses when the rhizobial infection processes are abolished in the epidermal cells (Pislariu *et al.*, 2012), the *nad1* nodules exhibited rapid and strong defense responses that resemble pathogen triggered HR-like cell death of both rhizobia and host cells, and the necrotic region occupied most of the symbiotic region of the nodules, which is reminiscent of the defense-like responses in *dnf2* nodules (Fig. S8). Therefore, *nad1* will serve as another good model for studying the maintenance of rhizobial endosymbiosis and prevention of plant defense-like responses in nodules. Moreover, it is interesting to test in which step NAD1 acts in the multiple step control of immunity during the intracellular accommodation of rhizobia (Berrabah *et al.*, 2015). Mitochondria play a central role in integrating multiple cell death signals (Lam *et al.*, 2001). In particular, changes in the redox state of mitochondria are important for cellular metabolic dysfunction leading to HR (Mur *et al.*, 2008), and may also be one of the reasons for observed defense responses, such as H_2O_2 accumulation, in *nad1* nodules (Fig. 6m). The increased concentration of H_2O_2 could kill the rhizobia directly or serve as a death signal leading to cell death. RBOH, an NADPH oxidase, has been shown to be a major ROS-generating system in plants (Marino *et al.*, 2012), and its transcript level was rapidly elevated in *nad1* nodule primordia. The *Rboh* detected in our results corresponds to *MtRbohC* described before, which was

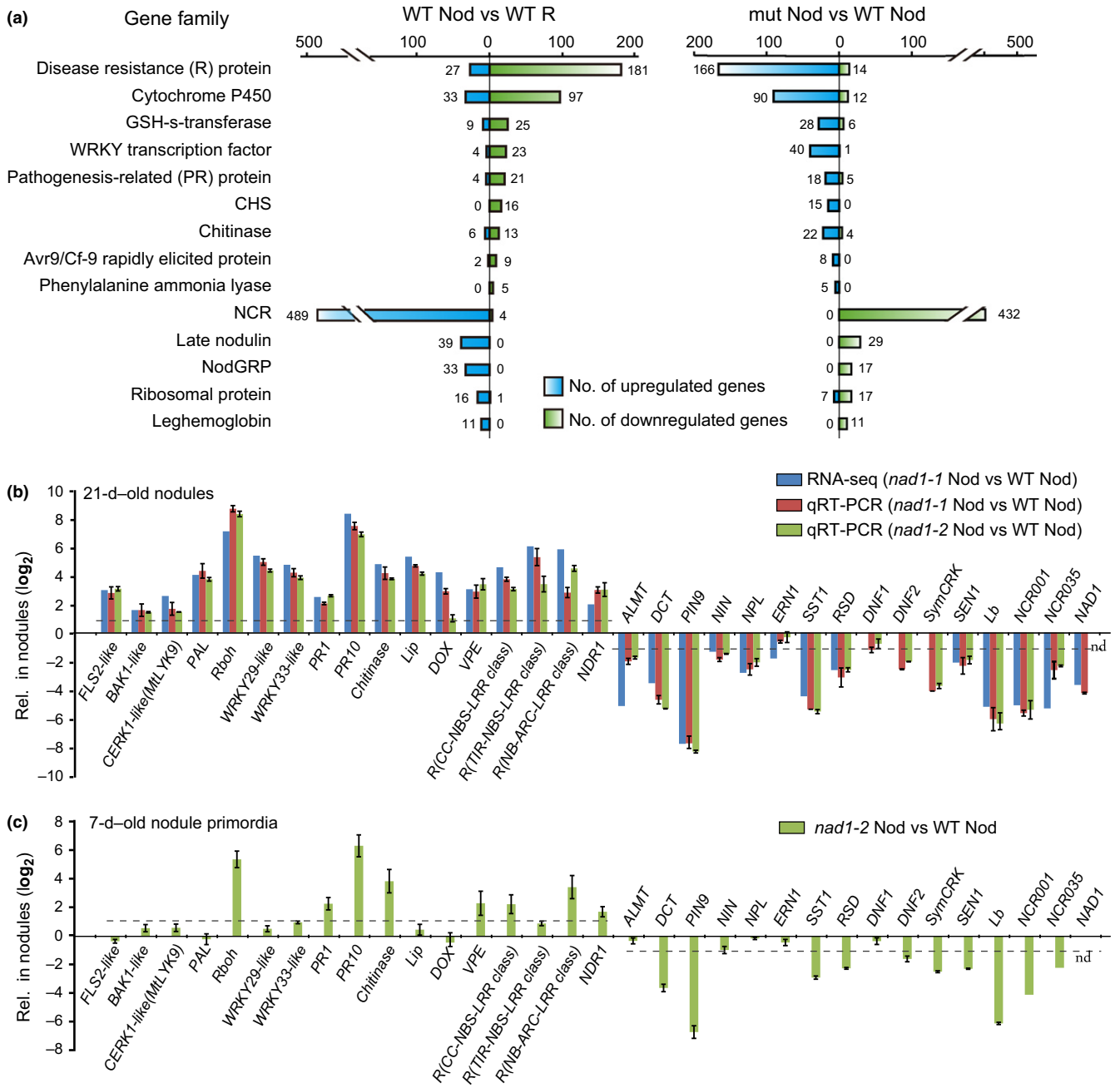

Fig. 7 Reprogramming of transcriptome of *nodules with activated defense 1* (*nad1*) nodules. (a) Comparison of transcription of gene families in wild-type nodules (WT Nod) vs WT nodule-stripped roots (WT R) (left panel) and *nad1-1* mutant nodules (mut Nod) vs WT Nod (right panel). Genes representing each family are highlighted in Supporting Information Tables S4 and S5. Values in front of bars indicate the numbers of genes in the family. (b, c) Analysis of representative differentially expressed genes (DEGs) was performed using total RNA from 21-d-old nodules (b), 7-d-old nodule primordia (c) for the *nad1* and WT *Medicago truncatula* R108 nodules. Upregulated genes in mut Nod vs WT Nod, related to defense, included the *PRR* gene *FLS2-like* and its co-receptor *BRASSINOSTEROIDS INSENSITIVE 1-associated receptor kinase 1-like* (*BAK1-like*), *CERK1-like*, *PAL*, *Rboh*, *WRKY29/33-like*, *PR*, *Chitinase*, *lignin biosynthetic peroxidase* (*Lip*), *pathogen-inducible alpha-dioxygenase* (*DOX*), *VPE*, *R* genes and *NDR1*(Kitajima & Sato, 1999; Piontek *et al.*, 2001; Hara-Nishimura *et al.*, 2005; Miya *et al.*, 2007; Gao *et al.*, 2009; Mao *et al.*, 2011; Samac *et al.*, 2011; Marino *et al.*, 2012; Vicente *et al.*, 2012; Nars *et al.*, 2013; Qi & Innes, 2013; Selote *et al.*, 2014). However, among the transcriptionally repressed genes in mut Nod vs WT Nod, the repression of *aluminum activated malate transporter* (*ALMT*) and *C4-dicarboxylate transporter* (*DCT*) genes indicated the impairment of carbon source transport (Batista *et al.*, 2001; Ligaba *et al.*, 2013). Other transcriptionally repressed genes included *NIN*, *NPL*, and *ERN1*, which have previously been reported to be required for development of infection threads and nodules, and *SST1*, *RSD*, *DNF1/2*, *SymCRK*, *SEN1*, *Lb* and *NCR001/035*, which are known to be required for nitrogen fixation, bacteroid differentiation and the symbiotic suppression of defense (Krusell *et al.*, 2005; Ott *et al.*, 2005; Marsh *et al.*, 2007; Middleton *et al.*, 2007; Van de Velde *et al.*, 2010; Wang *et al.*, 2010; Hakoyama *et al.*, 2012; Xie *et al.*, 2012; Bourcy *et al.*, 2013; Sinharoy *et al.*, 2013; Berrabah *et al.*, 2014b). Fold changes were calculated by the ratio of relative expression levels (Rel.) of genes in *nad1* mutant vs WT nodules. Error bars for (b, c) indicate ± SDs obtained from two biological replicates. See detailed information about selected genes in Table S1. NCR, nodule-specific cysteine-rich (NCR); CHS, chalcone synthase; qRT-PCR, quantitative reverse transcription polymerase chain reaction.

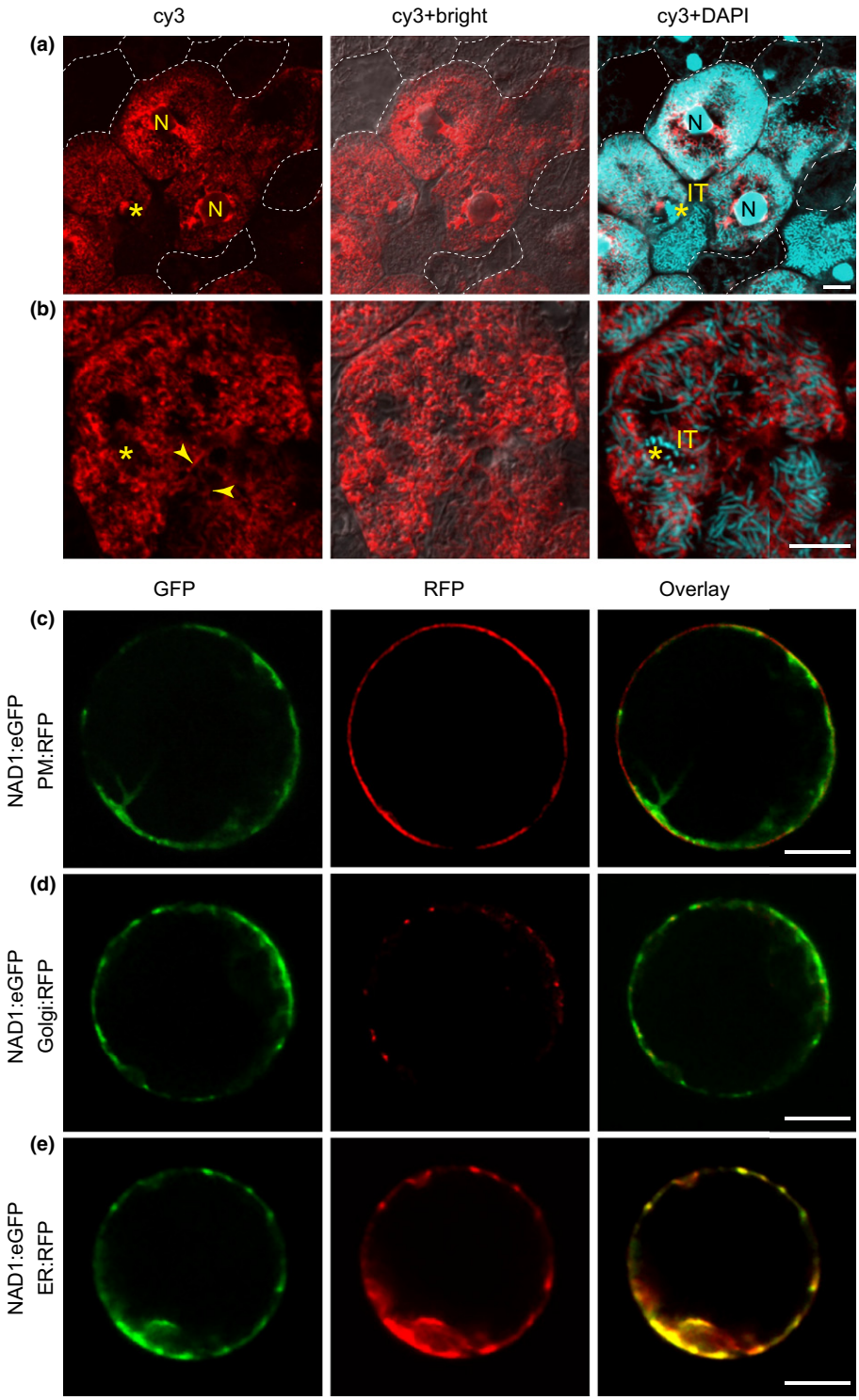

Fig. 8 Localization of nodules with activated defense 1 (NAD1). (a, b) *Medicago truncatula* NAD1 was fused to the N-terminus of 3 × flag tag and expressed under the control of its native promoter in *nad1-1* roots. Rescued nodules (pink nodules) were used for immunofluorescence assay by anti-flag antibody (Sigma) and fluorescence secondary antibody conjugated with Cy3 (red channel). Rhizobia were stained with 4′,6′-diamidino-2-phenylindol (DAPI). In noninfected cells, outlined with dotted lines, no clear signals were observed. In rhizobium-infected cells, NAD1 signals displayed endoplasmic reticulum (ER)-like structures (arrowheads), appeared elongated and closely associated with symbiosomes. Asterisks indicate the site of an infection thread (IT). N, nuclei. (c–e) NAD1 was fused to eGFP (green fluorescent protein (GFP) channel) and coexpressed with plasma membrane (PM), Golgi and ER localized markers (red fluorescent protein (RFP) channel) in *Arabidopsis* protoplasts. NAD1 was co-localized with ER marker but not PM or Golgi marker. Bars, 10 μm.

shown to be strictly controlled to a very low expression level in *Medicago* roots and nodules (Marino *et al.*, 2011).

Our RNA-seq data showed a striking transcriptomic reprogramming of the plant defense-related genes from 'suppression' in the wild-type to the 'activation' state in *nad1* nodules. Among plant defense-related genes induced in *nad1* mutants, *R* genes comprised the largest family (Fig. 7). During effector triggered immunity, R proteins recognize and bind specific bacterial effectors, and induce programmed cell death. R proteins from legumes can recognize effectors secreted from rhizobia, resulting in HR-like cell death for repulsing incompatible rhizobia and restricting the rhizobial host range (Yang *et al.*, 2010). Thus, repression of *R* genes in nodules may be one of the major plant strategies for host cells to tolerate the massive rhizobial colonization. By contrast, a large number of *R* genes were activated in *nad1* nodules, indicating the misregulation of the suppressed

defense in nodules. The transcriptional reprogramming was further confirmed for 7-d-old nodule primordia and corroborated by the observation that the defense responses were activated and endosymbiosis suppressed rapidly in the 7-d-old *nad1* nodule primordia.

NAD1 is not required for the early symbiosis stage, for example IT and nodule primordium formation. In *nad1*, rhizobia propagate and progress normally in ITs, but seem to be repulsed when they are released to symbiotic cells. Despite the strong and rapid defense responses that are observed in *nad1* nodule primordia, it is not clear whether ectopic defense responses trigger the defects in endosymbiosis, or, alternatively, the failure to properly establish the endosymbiosis-triggered defense responses. Moreover, the elevated defense responses that we detected may be a secondary/indirect effect of abnormal membrane trafficking and membrane biogenesis caused by dysfunction of ER-membrane localized NAD1. This uncertainty is the consequence of the biochemical and biological functions of NAD1 remaining unclear. NAD1 is a small ER-localized membrane protein. ER secretory pathway is reported to be particularly active in nodule zone II–III where NAD1 resides, suggesting that the ER secretory pathway is critical for the establishment of endosymbiosis (Maunoury *et al.*, 2010; Wang *et al.*, 2010). NAD1 might associate with the ER secretory pathway and then act to maintain the rhizobial endosymbiosis. NAD1 might also be involved in ER stress signaling linked to plant immunity (Kørner *et al.*, 2015). Both of these theories need to be tested in the future. In conclusion, our work opens up many interesting questions for a novel ER-localized transmembrane protein, existing in the genome of root nodule symbiosis plants, that functions in the maintenance of rhizobial endosymbiosis.

Acknowledgements

We thank: Dr Giles E. D. Oldroyd (John Innes Centre, UK) for kindly providing seeds of the symbiosis defective mutants *dmi1-1*, *dmi2-1*, *dmi3-1*, *nfp-1*, *nsp1-1* and *nsp2-2*; Dr Fang Xie (Shanghai Institute of Plant Physiology & Ecology) for providing *Rhizobium* strain Sm2011 expressing *lacZ*; the Samuel Roberts Noble Foundation for providing *Tnt1* insertion mutant seeds (NF18553 and NF14356); and Dr Dong Wang (University of Massachusetts Amherst, MA, USA) for providing *dnf2* mutant seeds (NF2496). This work was supported by the National Basic Research Program of China (973 program) (grant 2010C126502), the National Natural Science Foundation of China (grant 31370278), the Doctoral Program of Higher Education of China (grant 20130146130003) and the State Key Laboratory of Agricultural Microbiology (grant AMLKF200804). Generation of *M. truncatula Tnt1* insertion lines was funded by National Science Foundation Plant Genome Grants (DBI-0703285 and IOS-1127155).

Author contributions

C.W., Z.Z., L.L. and Z.H. planned and designed the research. C.W., H.Y., L.D., L.C., X.H., G.L. and A.X. performed the experiments. J.W. and K.S.M. screened and provided the *Tnt1* mutant lines. C.W. and Z.Z. analyzed the data. C.W. and Z.H. wrote the article with suggestions from D.D and Y.C.

References

Anders S, Huber W. 2010. Differential expression analysis for sequence count data. *Genome Biology* **11**: R106.

Anders S, Pyl PT, Huber W. 2015. HTSeq – a Python framework to work with high-throughput sequencing data. *Bioinformatics* **31**: 166–169.

Bagchi R, Salehin M, Adeyemo OS, Salazar C, Shulaev V, Sherrier DJ, Dickstein R. 2012. Functional assessment of the *Medicago truncatula* NIP/LATD protein demonstrates that it is a high-affinity nitrate transporter. *Plant Physiology* **160**: 906–916.

Banba M, Gutjahr C, Miyao A, Hirochika H, Paszkowski U, Kouchi H, Imaizumi-Anraku H. 2008. Divergence of evolutionary ways among common sym genes: *CASTOR* and *CCaMK* show functional conservation between two symbiosis systems and constitute the root of a common signaling pathway. *Plant & Cell Physiology* **49**: 1659–1671.

Batista S, Catalán AI, Hernández-Lucas I, Martínez-Romero E, Aguilar OM, Martínez-Drets G. 2001. Identification of a system that allows a *Rhizobium tropici dctA* mutant to grow on succinate, but not on other C_4-dicarboxylates. *Canadian Journal of Microbiology* **47**: 509–518.

Benedito VA, Torres-Jerez I, Murray JD, Andriankaja A, Allen S, Kakar K, Wandrey M, Verdier J, Zuber H, Ott T *et al.* 2008. A gene expression atlas of the model legume *Medicago truncatula*. *Plant Journal* **55**: 504–513.

Berrabah F, Bourcy M, Cayrel A, Eschstruth A, Mondy S, Ratet P, Gourion B. 2014a. Growth conditions determine the *DNF2* requirement for symbiosis. *PLoS ONE* **9**: e91866.

Berrabah F, Bourcy M, Eschstruth A, Cayrel A, Guefrachi I, Mergaert P, Wen J, Jean V, Mysore KS, Gourion B *et al.* 2014b. A nonRD receptor-like kinase prevents nodule early senescence and defense-like reactions during symbiosis. *New Phytologist* **203**: 1305–1314.

Berrabah F, Ratet P, Gourion B. 2015. Multiple steps control immunity during the intracellular accommodation of rhizobia. *Journal of Experimental Botany* **66**: 1977–1985.

Bolger AM, Lohse M, Usadel B. 2014. Trimmomatic: a flexible trimmer for Illumina sequence data. *Bioinformatics* **30**: 2114–2120.

Boscari A, Del Giudice J, Ferrarini A, Venturini L, Zaffini AL, Delledonne M, Puppo A. 2013. Expression dynamics of the *Medicago truncatula* transcriptome during the symbiotic interaction with *Sinorhizobium meliloti*: which role for nitric oxide? *Plant Physiology* **161**: 425–439.

Bourcy M, Brocard L, Pislariu CI, Cosson V, Mergaert P, Tadege M, Mysore KS, Udvardi MK, Gourion B, Ratet P. 2013. *Medicago truncatula* DNF2 is a PI-PLC-XD-containing protein required for bacteroid persistence and prevention of nodule early senescence and defense-like reactions. *New Phytologist* **197**: 1250–1261.

Cheng X, Wang M, Lee HK, Tadege M, Ratet P, Udvardi M, Mysore KS, Wen J. 2014. An efficient reverse genetics platform in the model legume *Medicago truncatula*. *New Phytologist* **201**: 1065–1076.

Desbrosses GJ, Stougaard J. 2011. Root nodulation: a paradigm for how plant–microbe symbiosis influences host developmental pathways. *Cell Host & Microbe* **10**: 348–358.

Domonkos A, Horvath B, Marsh JF, Halasz G, Ayaydin F, Oldroyd GE, Kalo P. 2013. The identification of novel loci required for appropriate nodule development in *Medicago truncatula*. *BMC Plant Biology* **13**: 157.

Downie JA. 2014. Legume nodulation. *Current Biology* **24**: R184–R190.

Gao M, Wang X, Wang D, Xu F, Ding X, Zhang Z, Bi D, Cheng YT, Chen S, Li X *et al.* 2009. Regulation of cell death and innate immunity by two receptor-like kinases in *Arabidopsis*. *Cell Host & Microbe* **6**: 34–44.

Gómez-Gómez L, Boller T. 2000. FLS2: an LRR receptor-like kinase involved in the perception of the bacterial elicitor flagellin in *Arabidopsis*. *Molecular Cell* **5**: 1003–1011.

Gourion B, Berrabah F, Ratet P, Stacey G. 2015. *Rhizobium*–legume symbioses: the crucial role of plant immunity. *Trends in Plant Science* **20**: 186–194.

Graham MA, Silverstein KA, Cannon SB, VandenBosch KA. 2004. Computational identification and characterization of novel genes from legumes. *Plant Physiology* **135**: 1179–1197.

Gyaneshwar P, James EK, Mathan N, Reddy PM, Reinhold-Hurek B, Ladha JK. 2001. Endophytic colonization of rice by a diazotrophic strain of *Serratia marcescens*. *Journal of Bacteriology* **183**: 2634–2645.

Hakoyama T, Niimi K, Yamamoto T, Isobe S, Sato S, Nakamura Y, Tabata S, Kumagai H, Umehara Y, Brossuleit K *et al.* 2012. The integral membrane protein SEN1 is required for symbiotic nitrogen fixation in *Lotus japonicus* nodules. *Plant & Cell Physiology* **53**: 225–236.

Hara-Nishimura I, Hatsugai N, Nakaune S, Kuroyanagi M, Nishimura M. 2005. Vacuolar processing enzyme: an executor of plant cell death. *Current Opinion in Plant Biology* **8**: 404–408.

Hayashi M, Parniske M. 2014. Symbiosis and pathogenesis: what determines the difference? *Current Opinion in Plant Biology* **20**: v–vi.

He J, Benedito VA, Wang M, Murray JD, Zhao PX, Tang Y, Udvardi MK. 2009. The *Medicago truncatula* gene expression atlas web server. *BMC Bioinformatics* **10**: 441.

Kitajima S, Sato F. 1999. Plant pathogenesis-related proteins: molecular mechanisms of gene expression and protein function. *Journal of Biochemistry* **125**: 1–8.

Kørner CJ, Du X, Vollmer ME, Pajerowska-Mukhtar KM. 2015. Endoplasmic reticulum stress signaling in plant immunity – at the crossroad of life and death. *International Journal of Molecular Sciences* **16**: 26 582–26 598.

Kouchi H, Shimomura K, Hata S, Hirota A, Wu GJ, Kumagai H, Tajima S, Suganuma N, Suzuki A, Aoki T *et al.* 2004. Large-scale analysis of gene expression profiles during early stages of root nodule formation in a model legume, *Lotus japonicus*. *DNA Research* **11**: 263–274.

Krusell L, Krause K, Ott T, Desbrosses G, Kramer U, Sato S, Nakamura Y, Tabata S, James EK, Sandal N *et al.* 2005. The sulfate transporter SST1 is crucial for symbiotic nitrogen fixation in *Lotus japonicus* root nodules. *Plant Cell* **17**: 1625–1636.

Lam E, Kato N, Lawton M. 2001. Programmed cell death, mitochondria and the plant hypersensitive response. *Nature* **411**: 848–853.

Leong SA, Williams PH, Ditta GS. 1985. Analysis of the 5′ regulatory region of the gene for delta-aminolevulinic acid synthetase of *Rhizobium meliloti*. *Nucleic Acids Research* **13**: 5965–5976.

Li H, Handsaker B, Wysoker A, Fennell T, Ruan J, Homer N, Marth G, Abecasis G, Durbin R, Genome Project Data Processing Subgroup. 2009. The Sequence Alignment/Map format and SAMtools. *Bioinformatics* **25**: 2078–2079.

Li X, Xu J, Yu G, Luo L. 2012. A wound-induced small polypeptide gene family is upregulated in soybean nodules. *Chinese Science Bulletin* **58**: 1003–1009.

Ligaba A, Dreyer I, Margaryan A, Schneider DJ, Kochian L, Piñeros M. 2013. Functional, structural and phylogenetic analysis of domains underlying the Al sensitivity of the aluminum-activated malate/anion transporter, TaALMT1. *Plant Journal* **76**: 766–780.

Limpens E, Ramos J, Franken C, Raz V, Compaan B, Franssen H, Bisseling T, Geurts R. 2004. RNA interference in *Agrobacterium rhizogenes*-transformed roots of *Arabidopsis* and *Medicago truncatula*. *Journal of Experimental Botany* **55**: 983–992.

Loiret FG, Ortega E, Kleiner D, Ortega-Rodés P, Rodés R, Dong Z. 2004. A putative new endophytic nitrogen-fixing bacterium *Pantoea* sp. from sugarcane. *Journal of Applied Microbiology* **97**: 504–511.

Mao G, Meng X, Liu Y, Zheng Z, Chen Z, Zhang S. 2011. Phosphorylation of a WRKY transcription factor by two pathogen-responsive MAPKs drives phytoalexin biosynthesis in *Arabidopsis*. *Plant Cell* **23**: 1639–1653.

Marino D, Andrio E, Danchin EG, Oger E, Gucciardo S, Lambert A, Puppo A, Pauly N. 2011. A *Medicago truncatula* NADPH oxidase is involved in symbiotic nodule functioning. *New Phytologist* **189**: 580–592.

Marino D, Dunand C, Puppo A, Pauly N. 2012. A burst of plant NADPH oxidases. *Trends in Plant Science* **17**: 9–15.

Markmann K, Parniske M. 2009. Evolution of root endosymbiosis with bacteria: how novel are nodules? *Trends in Plant Science* **14**: 77–86.

Marsh JF, Rakocevic A, Mitra RM, Brocard L, Sun J, Eschstruth A, Long SR, Schultze M, Ratet P, Oldroyd GE. 2007. *Medicago truncatula NIN* is essential for rhizobial-independent nodule organogenesis induced by autoactive calcium/calmodulin-dependent protein kinase. *Plant Physiology* **144**: 324–335.

Maunoury N, Redondo-Nieto M, Bourcy M, Van de Velde W, Alunni B, Laporte P, Durand P, Agier N, Marisa L, Vaubert D *et al.* 2010. Differentiation of symbiotic cells and endosymbionts in *Medicago truncatula* nodulation are coupled to two transcriptome-switches. *PLoS ONE* **5**: e9519.

Meng X, Zhang S. 2013. MAPK cascades in plant disease resistance signaling. *Annual Review of Phytopathology* **51**: 245–266.

Middleton PH, Jakab J, Penmetsa RV, Starker CG, Doll J, Kalo P, Prabhu R, Marsh JF, Mitra RM, Kereszt A *et al.* 2007. An ERF transcription factor in *Medicago truncatula* that is essential for Nod factor signal transduction. *Plant Cell* **19**: 1221–1234.

Miya A, Albert P, Shinya T, Desaki Y, Ichimura K, Shirasu K, Narusaka Y, Kawakami N, Kaku H, Shibuya N. 2007. CERK1, a LysM receptor kinase, is essential for chitin elicitor signaling in *Arabidopsis*. *Proceedings of the National Academy of Sciences, USA* **104**: 19 613–19 618.

Moreau S, Verdenaud M, Ott T, Letort S, de Billy F, Niebel A, Gouzy J, de Carvalho-Niebel F, Gamas P. 2011. Transcription reprogramming during root nodule development in *Medicago truncatula*. *PLoS ONE* **6**: e16463.

Mur LA, Kenton P, Lloyd AJ, Ougham H, Prats E. 2008. The hypersensitive response; the centenary is upon us but how much do we know? *Journal of Experimental Botany* **59**: 501–520.

Muthamilarasan M, Prasad M. 2013. Plant innate immunity: an updated insight into defense mechanism. *Journal of Biosciences* **38**: 433–449.

Nars A, Rey T, Lafitte C, Vergnes S, Amatya S, Jacquet C, Dumas B, Thibaudeau C, Heux L, Bottin A *et al.* 2013. An experimental system to study responses of *Medicago truncatula* roots to chitin oligomers of high degree of polymerization and other microbial elicitors. *Plant Cell Reports* **32**: 489–502.

Oldroyd GE. 2013. Speak, friend, and enter: signalling systems that promote beneficial symbiotic associations in plants. *Nature Reviews: Microbiology* **11**: 252–263.

Ott T, van Dongen JT, Günther C, Krusell L, Desbrosses G, Vigeolas H, Bock V, Czechowski T, Geigenberger P, Udvardi MK. 2005. Symbiotic leghemoglobins are crucial for nitrogen fixation in legume root nodules but not for general plant growth and development. *Current Biology* **15**: 531–535.

Piontek K, Smith AT, Blodig W. 2001. Lignin peroxidase structure and function. *Biochemical Society Transactions* **29**: 111–116.

Pislariu CI, Murray JD, Wen J, Cosson V, Muni RR, Wang M, Benedito VA, Andriankaja A, Cheng X, Jerez IT *et al.* 2012. A *Medicago truncatula* tobacco retrotransposon insertion mutant collection with defects in nodule development and symbiotic nitrogen fixation. *Plant Physiology* **159**: 1686–1699.

Qi D, Innes RW. 2013. Recent advances in plant NLR structure, function, localization, and signaling. *Frontiers in Immunology* **4**: 348.

Roux B, Rodde N, Jardinaud MF, Timmers T, Sauviac L, Cottret L, Carrère S, Sallet E, Courcelle E, Moreau S *et al.* 2014. An integrated analysis of plant and bacterial gene expression in symbiotic root nodules using laser-capture microdissection coupled to RNA sequencing. *Plant Journal* **77**: 817–837.

Saeki K. 2011. Rhizobial measures to evade host defense strategies and endogenous threats to persistent symbiotic nitrogen fixation: a focus on two legume–rhizobium model systems. *Cellular and Molecular Life Sciences* **68**: 1327–1339.

Samac DA, Peñuela S, Schnurr JA, Hunt EN, Foster-Hartnett D, Vandenbosch KA, Gantt JS. 2011. Expression of coordinately regulated defence response genes and analysis of their role in disease resistance in *Medicago truncatula*. *Molecular Plant Pathology* **12**: 786–798.

Sandhiya GS, Sugitha TC, Balachandar D, Kumar K. 2005. Endophytic colonization and *in planta* nitrogen fixation by a diazotrophic *Serratia* sp. in rice. *Indian Journal of Experimental Biology* **43**: 802–807.

Selote D, Shine MB, Robin GP, Kachroo A. 2014. Soybean NDR1-like proteins bind pathogen effectors and regulate resistance signaling. *New Phytologist* **202**: 485–498.

Sinharoy S, Torres-Jerez I, Bandyopadhyay K, Kereszt A, Pislariu CI, Nakashima J, Benedito VA, Kondorosi E, Udvardi MK. 2013. The C_2H_2 transcription factor regulator of symbiosome differentiation represses transcription of the secretory pathway gene *VAMP721a* and promotes symbiosome development in *Medicago truncatula*. *Plant Cell* **25**: 3584–3601.

Soto MJ, Domínguez-Ferreras A, Pérez-Mendoza D, Sanjuán J, Olivares J. 2009. Mutualism versus pathogenesis: the give-and-take in plant–bacteria interactions. *Cellular Microbiology* **11**: 381–388.

Soyano T, Hayashi M. 2014. Transcriptional networks leading to symbiotic nodule organogenesis. *Current Opinion in Plant Biology* **20**: 146–154.

Svistoonoff S, Hocher V, Gherbi H. 2014. Actinorhizal root nodule symbioses: what is signalling telling on the origins of nodulation? *Current Opinion in Plant Biology* **20C**: 11–18.

Tadege M, Wen J, He J, Tu H, Kwak Y, Eschstruth A, Cayrel A, Endre G, Zhao PX, Chabaud M *et al.* 2008. Large-scale insertional mutagenesis using the *Tnt1* retrotransposon in the model legume *Medicago truncatula*. *Plant Journal* **54**: 335–347.

Udvardi M, Poole PS. 2013. Transport and metabolism in legume–rhizobia symbioses. *Annual Review of Plant Biology* **64**: 781–805.

Van de Velde W, Zehirov G, Szatmari A, Debreczeny M, Ishihara H, Kevei Z, Farkas A, Mikulass K, Nagy A, Tiricz H *et al.* 2010. Plant peptides govern terminal differentiation of bacteria in symbiosis. *Science* **327**: 1122–1126.

Vasse J, de Billy F, Camut S, Truchet G. 1990. Correlation between ultrastructural differentiation of bacteroids and nitrogen fixation in alfalfa nodules. *Journal of Bacteriology* **172**: 4295–4306.

Vicente J, Cascón T, Vicedo B, Garcia-Agustín P, Hamberg M, Castresana C. 2012. Role of 9-lipoxygenase and alpha-dioxygenase oxylipin pathways as modulators of local and systemic defense. *Molecular Plant* **5**: 914–928.

Wang C, Zhu M, Duan L, Yu H, Chang X, Li L, Kang H, Feng Y, Zhu H, Hong Z *et al.* 2015. *Lotus japonicus* Clathrin Heavy Chain1 is associated with Rho-Like GTPase ROP6 and involved in nodule formation. *Plant Physiology* **167**: 1497–1510.

Wang D, Griffitts J, Starker C, Fedorova E, Limpens E, Ivanov S, Bisseling T, Long S. 2010. A nodule-specific protein secretory pathway required for nitrogen-fixing symbiosis. *Science* **327**: 1126–1129.

Wang X, Cai Y, Wang H, Zeng Y, Zhuang X, Li B, Jiang L. 2014. *Trans*-Golgi network-located AP1 gamma adaptins mediate dileucine motif-directed vacuolar targeting in *Arabidopsis*. *Plant Cell* **26**: 4102–4118.

Xie F, Murray JD, Kim J, Heckmann AB, Edwards A, Oldroyd GE, Downie JA. 2012. Legume pectate lyase required for root infection by rhizobia. *Proceedings of the National Academy of Sciences, USA* **109**: 633–638.

Yang S, Tang F, Gao M, Krishnan HB, Zhu H. 2010. *R* gene-controlled host specificity in the legume–rhizobia symbiosis. *Proceedings of the National Academy of Sciences, USA* **107**: 18735–18740.

Young ND, Debelle F, Oldroyd GE, Geurts R, Cannon SB, Udvardi MK, Benedito VA, Mayer KF, Gouzy J, Schoof H *et al.* 2011. The *Medicago* genome provides insight into the evolution of rhizobial symbioses. *Nature* **480**: 520–524.

Supporting Information

Additional Supporting Information may be found online in the Supporting Information tab for this article:

Fig. S1 Expression profiles of *MtNAD1* and *LjNAD1* gene in the databases MtGEA and LjGEA.

Fig. S2 Plant growth and nitrogen fixation phenotypes of *nad1* plants.

Fig. S3 Co-segregation of nodule phenotypes with the *nad1* genometypes in progenies of a heterozygous *nad1*/+ plant.

Fig. S4 The SEM of the wild-type and nad1 nodules.

Fig. S5 Infection threads and nodule primordia of the wild-type and *nad1-1* plants.

Fig. S6 Ultrastructures of the wild-type and *nad1* nodules.

Fig. S7 Phenolic compound staining and TUNEL assay at 14 dpi.

Fig. S8 Nodules formed in *dnf2* and *nad1* mutant plants.

Fig. S9 Complementation of *nad1-1* by the microbe *NAD1*-like gene.

Table S1 Analysis of gene expression profiles by qRT-PCR

Table S2 Constructs and primers

Table S3 NAD1 and NAD1-like peptide sequences

Table S4 Differentially expressed genes in nodules vs nodule-stripped roots of the wild-type plants

Table S5 Differentially expressed genes in *nad1* nodules vs the wild-type nodules

Please note: Wiley Blackwell are not responsible for the content or functionality of any Supporting Information supplied by the authors. Any queries (other than missing material) should be directed to the *New Phytologist* Central Office.